

Accepted Manuscript

Unveiling Novel Diphenyl-1*H*-pyrazole Based Acrylates Tethered to 1,2,3-Triazole as Promising Apoptosis Inducing Cytotoxic and Anti-inflammatory Agents

Mohammed Faraz Khan, Tarique Anwer, Afroz Bakht, Garima Verma, Wasim Akhtar, M Mumtaz Alam, Moshahid Alam Rizvi, Mymoona Akhter, Mohammad Shaquiquzzaman

PII: S0045-2068(18)31310-5
DOI: <https://doi.org/10.1016/j.bioorg.2019.03.071>
Reference: YBIOO 2897

To appear in: *Bioorganic Chemistry*

Received Date: 13 November 2018
Revised Date: 27 March 2019
Accepted Date: 27 March 2019

Please cite this article as: M. Faraz Khan, T. Anwer, A. Bakht, G. Verma, W. Akhtar, M. Mumtaz Alam, M. Alam Rizvi, M. Akhter, M. Shaquiquzzaman, Unveiling Novel Diphenyl-1*H*-pyrazole Based Acrylates Tethered to 1,2,3-Triazole as Promising Apoptosis Inducing Cytotoxic and Anti-inflammatory Agents, *Bioorganic Chemistry* (2019), doi: <https://doi.org/10.1016/j.bioorg.2019.03.071>

This is a PDF file of an unedited manuscript that has been accepted for publication. As a service to our customers we are providing this early version of the manuscript. The manuscript will undergo copyediting, typesetting, and review of the resulting proof before it is published in its final form. Please note that during the production process errors may be discovered which could affect the content, and all legal disclaimers that apply to the journal pertain.



Unveiling Novel Diphenyl-1*H*-pyrazole Based Acrylates Tethered to 1,2,3-Triazole as Promising Apoptosis Inducing Cytotoxic and Anti-inflammatory Agents

Mohammed Faraz Khan¹, Tarique Anwer², Afroz Bakht³, Garima Verma¹, Wasim Akhtar¹,
M Mumtaz Alam¹, Moshahid Alam Rizvi⁴, Mymoona Akhter¹, Mohammad
Shaquiquzzaman^{1*}

¹Drug Design and Medicinal Chemistry Lab, Department of Pharmaceutical Chemistry, School of
Pharmaceutical Education and Research, Jamia Hamdard, New Delhi 110062, India.

²Department of Pharmacology, College of Pharmacy, Jazan University, PO Box 114, Gizan, KSA.

³Department of Chemistry, College of Science and Humanities, Prince Sattam bin Abdulaziz
University, P.O. Box- 173, Al-Kharj, Saudi Arabia.

⁴The Genome Biology Lab, Department of Biosciences, Jamia Millia Islamia, New Delhi 110025,
India.

*Corresponding Author

Dr. Mohammad Shaquiquzzaman

Assistant Professor

Department of Pharmaceutical Chemistry

School of Pharmaceutical Education and Research

Jamia Hamdard, New Delhi-110062

Email: shaqiq@gmail.com

+91-9990663405

Abstract

Meagre and suboptimal therapeutic response along with the side effect profile associated with the existing anticancer therapy have necessitated the development of new therapeutic modalities to curb this disease. Bearing in mind the current scenario, a series of 1,2,3-triazole linked 3-(1,3-diphenyl-1*H*-pyrazol-4-yl)acrylates was synthesized following a multi-step reaction scheme. Initial screening for anticancer potential was done by *in vitro* sulforhodamine B assay against four human cancer cell lines- MCF-7 (breast), A549 (Lung) and HCT-116 and HT-29 (Colon). On evaluation, several compounds showed promising growth inhibition against all the cell lines, particularly compounds **6e**, **6f** and **6n**. Among them, compound **6f** displayed IC₅₀ values of 1.962, 3.597, 1.764 and 4.496 μ M against A549, HCT-116, MCF-7 and HT-29 cell lines respectively. Furthermore, the apoptosis inducing potential of the compounds was determined by Hoechst staining and DNA fragmentation assay. Colony formation inhibition assay was also carried out to determine the long term cytotoxic potential of the molecules. Moreover, compounds **6e**, **6f** and **6n** were also evaluated for anti-inflammatory activity by protein albumin denaturation assay and red blood cell membrane stabilizing assay.

Key Words

1,2,3-Triazole; Diphenyl Pyrazole; Acrylates; Anticancer; Apoptosis; Anti-inflammatory.

List of Abbreviations

Copper (II) sulphate pentahydrate	CuSO ₄ .5H ₂ O
Doublet	d
Dichloromethane	DCM
<i>N-N</i> -Dimethyl formamide	DMF
Dimethyl sulfoxide	DMSO
Equipped with Electrospray	ESI
<i>Hertz</i>	<i>Hz</i>
Half Maximal Inhibitory Concentration	IC ₅₀
Infra-red	IR

Coupling Constant	<i>J</i>
Multiplet	m
National Cancer Institute	NCI
Nuclear Magnetic Resonance	NMR
Non-Steroidal Anti-Inflammatory Drugs	NSAIDs
Protein Data Bank ID	PDB ID
Phosphorus Oxychloride	POCl ₃
<i>Parts Per Million</i>	ppm
<i>p</i> -Toluenesulfonic acid	<i>p</i> -TsOH
Research Collaboratory for Structural Bioinformatics	RCSB
Singlet	s
Standard Precision	SP
Sulforhodamine B	SRB
Triplet	t
Thin Layer Chromatography	TLC
Tetramethylsilane	TMS

1. Introduction

Cancer, a broad term used to characterize uncontrolled proliferation of cells arising from disruption or dysfunction of regulatory signalling pathways, which are normally under tight control, is one of the foremost diseases responsible for worldwide mortality [1]. At present, it is the major public concerned hotspot across the globe [2]. Deaths due to cancer are projected to continue rising with an approximate 3 million deaths in 2030 [3]. In developing and underdeveloped countries, lung, colon, breast and melanoma cancers are the most commonly reported cases [4]. However, emergence and spread of resistance to the currently available chemotherapeutic agents vindicates an urgent need for development of novel, more potent and selective anticancer agents [5].

Inflammation is a well-known phenomenon that an organism utilizes for resolving infections, tissue injury or restoring tissue functions *via* repair mechanism [6]. This response acts as a double-edged response [7]. Acute inflammation is an immediate response produced in response to tissue damage, which is generally useful for maintenance of homeostasis. This plays a beneficial role in protection against injury. However, chronic inflammation *i.e.* uncontrolled inflammatory reactions serve as a common etiologic factor for different ailments including cancer [8-10].

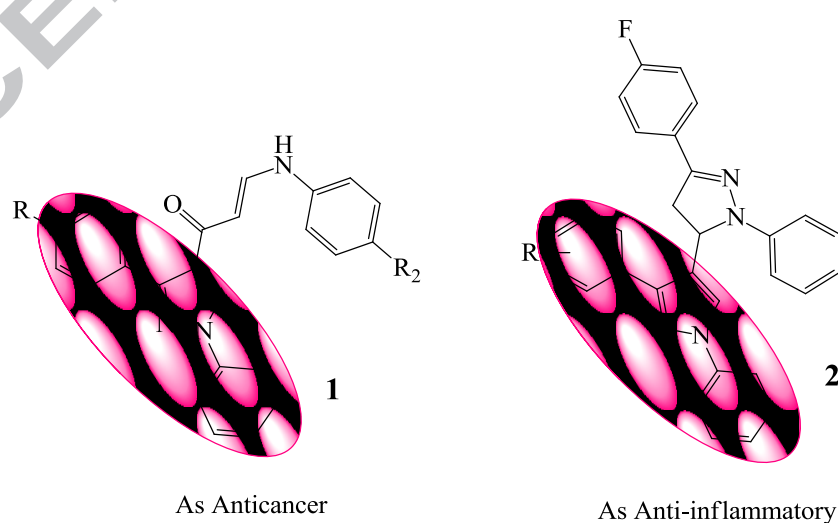
Link between chronic inflammation and cancer may be associated with different mechanisms like genomic instability induction, enhanced proliferation, inappropriate gene expression, resistance to apoptosis, metastasis, invasion through tumor-associated basement membrane, aggressive tumor neovascularization, etc. Elevated levels of reactive oxygen and nitrogen species can serve as major contributors in malignant cell transformation. Abnormal activation or overexpression of certain pro-inflammatory mediators like chemokines, cytokines, prostaglandins, cyclooxygenase-2, nitric oxide and inducible nitric oxide synthase promote tumor growth and progression. Certain pro-inflammatory mediators, particularly cytokines, chemokines and prostaglandins are known to endorse angiogenesis, thereby leading to metastasis and invasion [11].

Chronic inflammation plays a multifaceted role in carcinogenesis. Evidences from preclinical and clinical studies suggest that persistent inflammation functions as a driving force in the journey of cancer [12]. The inflammatory component contributes to tumor proliferation, angiogenesis, metastasis and resistance to hormonal and chemotherapy [13]. Chronic inflammation is also involved in the pathogenesis of insulin resistance, atherosclerosis,

neurodegeneration and tumor growth [14]. Work reported by Aleksandrova *et al.* provides an evidence that elevated CRP concentrations (markers of inflammation) are related to a higher risk of colon cancer [15]. Except for few drugs, long term use of anti-inflammatory drugs including non-steroidal anti-inflammatory drugs (NSAIDs) results in adverse effects such as bleeding, gastrointestinal ulceration and kidney damage [16].

Pyrazole moiety can be traced in number of anticancer agents *viz.* Crizotinib, Tartrazine, Pyrazomycin, etc. [17]. This moiety is found in a number of anti-inflammatory drugs also. To mention, these are Celecoxib, Ramifenazone, Deracoxib, Lonazolac, etc. [18]. Similarly, triazole bearing compounds are also known to exhibit potent anticancer (Anastrozole, Letrozole, Vorozole) and anti-inflammatory (Carboxyamidotriazole) activities [19]. Several pyrazole [20,21] and triazole [22,23] bearing agents reported in literature possess dual activity *i.e.*, anticancer and anti-inflammatory.

The diphenyl pyrazole moiety is receiving significant attention now a days, as the structural scaffold is found to make up the core structure of numerous anticancer (**1**) [24] and anti-inflammatory (**2**) [25] agents. Recent literature is enriched with progressive findings on anticancer (**3**) [26] and anti-inflammatory (**4**) [27] effects of 1,2,3-Triazole based compounds. Hybrids of diphenyl-pyrazole and 1,2,3-triazole were also reported as both anticancer (**5** and **6**) [28, 29] and anti-inflammatory (**7**) [30] agents recently. Several studies also revealed the anticancer (**8, 9**) [31, 32] and anti-inflammatory (**10**) [33] potential of acrylic acid derivatives, particularly the acrylates (**Figure 1**).



(a) Diphenyl Pyrazole Containing Compounds

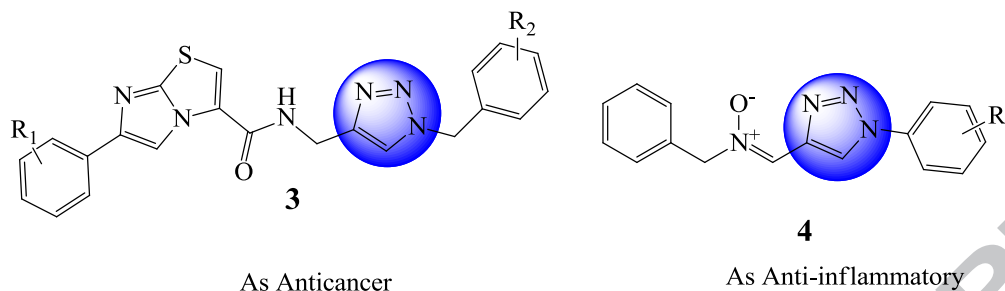
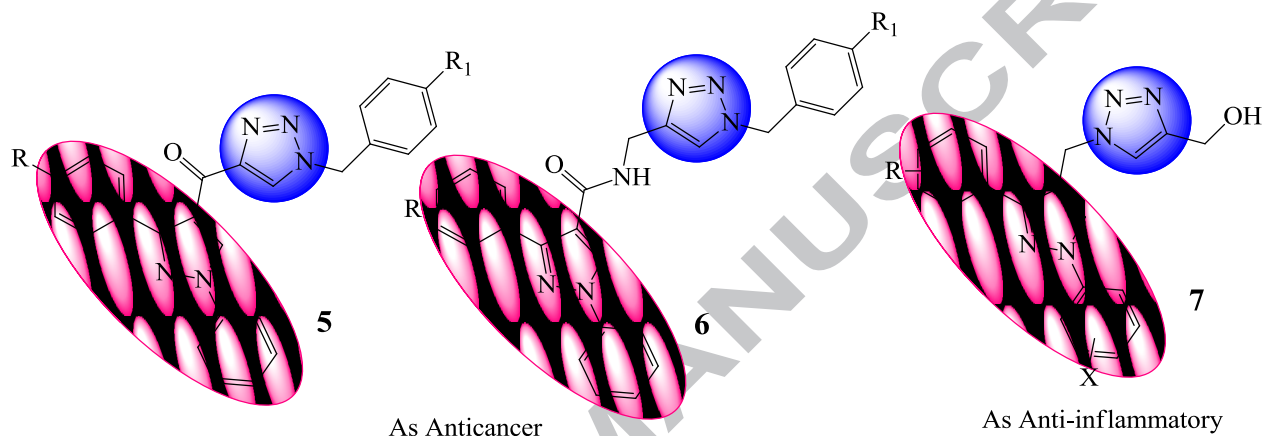
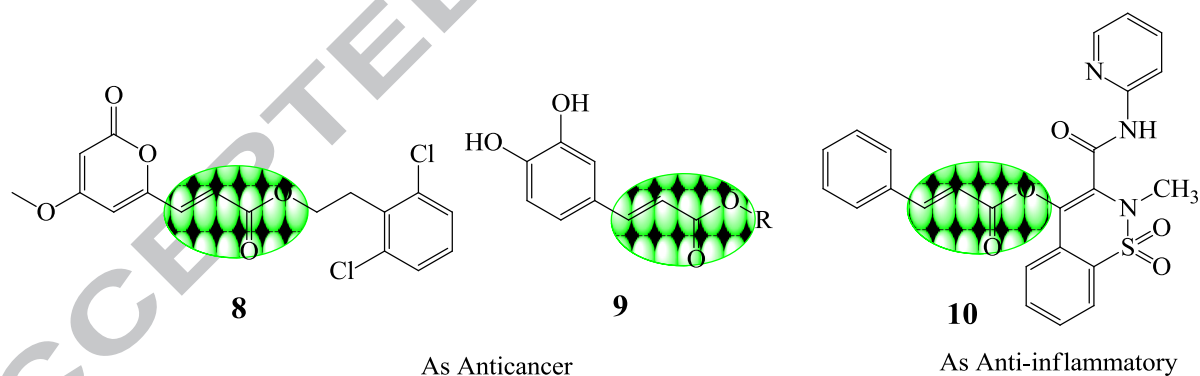
**(b) 1,2,3-Triazole Containing Compounds****(c) Diphenyl Pyrazole and 1,2,3-Triazole Containing Compounds****(d) Acrylate Linkage Containing Compounds**

Figure 1: Anticancer and anti-inflammatory compounds bearing (a) diphenyl pyrazole, (b) 1,2,3-triazole, (c) diphenyl pyrazole and 1,2,3-triazole and (d) acrylate linkage.

Despite significant potency of acrylic linkage, literature search revealed that diphenyl pyrazol-4-yl acrylic acid's analogs are found to be rarely synthesized [34] and never found to be clubbed with 1,2,3-triazoles. Henceforth, the present work reports synthesis of novel 3-(1,3-diphenyl-1*H*-pyrazol-4-yl)acrylates linked with 1,2,3-Triazole (**Figure 2**). The

synthesized molecules were evaluated for their anticancer and anti-inflammatory activities. On evaluation, several compounds were found to be potent against both cancer and inflammation.

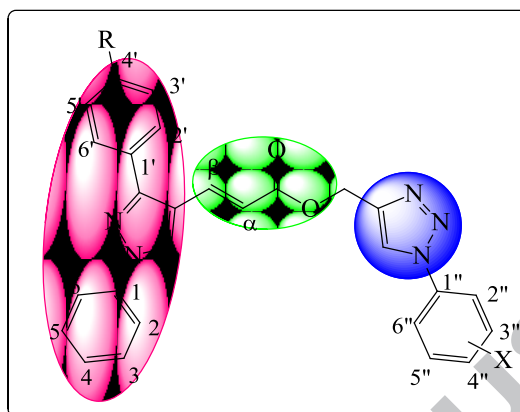


Figure 2: Structure of title compounds (Scheme 1).

2. Results and Discussion

2.1 Chemistry

Requisite compounds for **Scheme I** were obtained by employing multi-step reactions. Several substituted acetophenones were subjected to addition reaction with phenylhydrazine in the presence of glacial acetic acid. Subsequently, utilizing Vilsmeier-Haack reaction, formation of the pyrazole ring took place in the presence of *N,N*-dimethyl formamide (DMF) and phosphorus oxychloride (POCl_3). DMF served as acylating agent while POCl_3 acted as activating agent. Vilsmeier reagent, also known as Vilsmeier complex was formed during this reaction [35]. An aldol condensation's modified form, Knoevenagel condensation reaction was used to convert pyrazole carbaldehydes into pyrazole carboxylic acids. In this, aldehyde derivatives were reacted with malonic acid in the presence of pyridine and piperidine. In this reaction, pyridine was used as the solvent whereas piperidine served as the catalyst. This reaction is based on nucleophilic addition between an active hydrogen compound (malonic acid in this case) and an aldehyde, resulting in the formation of α,β -unsaturated dicarboxylic acid [36]. Furthermore, monocarboxylic acid derivatives were obtained by decarboxylation of dicarboxylic acids *via* Doebner modification [37]. The acids were further reacted with propargyl bromide in the presence of potassium carbonate to yield terminal alkyne bearing pyrazole acrylate derivatives [38].

Aromatic azides were formed in high yields by aromatic amines *via* diazotization with sodium nitrite in water in the presence of *p*-toluenesulfonic acid (*p*-TsOH) and subsequent addition of sodium azide [39].

These synthesized terminal alkyne bearing pyrazole acrylates and aromatic azides were coupled in the final step in the presence of catalytic copper (II) sulphate pentahydrate (CuSO₄·5H₂O) and sodium ascorbate in a H₂O/Dichloromethane (DCM) mixture at room temperature to yield the final compounds, triazoles [40].

2.2 Spectral Characterization

Spectral data for all the synthesized derivatives was found to be in concordance with the reported data and is discussed in detail in the **Supporting Information** section.

2.3 Biological Activity

Anticancer potential was assessed of all the prepared compounds (**4a-e**, **6a-o**). For assessing anticancer potential, the synthesized compounds were screened against a panel of four human cancer cell lines using the sulforhodamine B assay. Three of the most active compounds (**6e**, **6f** and **6n**) were further subjected to mechanistic studies including colony formation inhibition assay, Hoechst staining and DNA fragmentation assay.

Based on the reported facts that there exists a crucial link between cancer and inflammation. We also moved on the same aisle and got our most potent anticancer compounds (**6e**, **6f** and **6n**) evaluated for anti-inflammatory potential as well. Anti-inflammatory activity was performed using protein albumin denaturation assay and red blood cell membrane stabilizing assay.

2.3.1 Anticancer

2.3.1.1 Sulforhodamine B Assay

The newly synthesized compounds (**4a-e** and **6a-o**) were assessed for their *in vitro* cytotoxic potential against a panel of four human cancer cell lines *i.e.*, MCF-7 (breast), A549 (Lung) and HCT-116 and HT-29 (Colon).

Initial anticancer screening was performed at concentration of 1 and 10 μM (**Table 1**, **Supplementary Information**). The results of the preliminary anticancer screening were found to be in concordance with results of *in silico* studies. Half maximal inhibitory

concentration (IC_{50}) value was determined for the compounds showing more than 50% inhibition at a concentration of 10 μ M. Amongst the compounds of this series, compounds **6e**, **6f** and **6n** were tested at concentrations of 1, 3, 5, 7 and 10 μ M in order to determine IC_{50} values against the aforementioned panel of cell lines. On evaluation, compound **6f** emerged as the most active compound with IC_{50} values of 1.962, 3.597, 1.764 and 4.496 μ M against A549, HCT-116, MCF-7 and HT-29 respectively. Another compound, **6n** also displayed promising activity profile against HCT-116, MCF-7 and HT-29 with IC_{50} values of 4.940, 1.851 and 4.362 μ M respectively (**Table 1**). Depending on the results, colony formation inhibition assay, DNA fragmentation assay and fluorescence microscopy studies were also performed for compounds **6e**, **6f** and **6n**.

Table 1: IC_{50} values of compounds **6e**, **6f** and **6n** against a panel of Human Cancer Cell Lines

Cell Line Type		A549	HCT-116	MCF-7	HT-29
Tissue		Lung	Colon	Breast	Colon
S.No.	Compd.	IC_{50} μ M			
1.	6e	10.607 \pm 0.08	15.159 \pm 0.34	10.184 \pm 0.24	8.629 \pm 0.20
2.	6f	1.962 \pm 0.16	3.597 \pm 0.26	1.764 \pm 0.18	4.496 \pm 0.26
3.	6n	9.463 \pm 0.24	4.940 \pm 0.45	1.851 \pm 0.42	4.362 \pm 0.13
4.	Camptothecin	0.030 \pm 0.17	0.050 \pm 0.14	0.200 \pm 0.24	0.800 \pm 0.27
5.	Combretastatin A4	0.180 \pm 0.22	0.006 \pm 0.06	0.033 \pm 0.26	>10

2.3.1.2 Colony formation inhibition assay

Clonogenic cell survival assay is performed to assess the ability of a single cell to grow into a colony. It helps us in investigating the long term cytotoxic potential. Since the method reflects all modes of cell death or arrest, it is considered to be a standard for determining long term cell viability [41]. The colony formation of MCF-7 cells was found to be significantly inhibited by the exposure of MCF-7 cells to the compounds (**Figure 3**). The clonogenic cell survival is found to be reduced approximately to its half, and was found to be in agreement with IC_{50} values of the compounds. The result indicates that the molecules can efficiently inhibit proliferation and growth of MCF-7 cells.

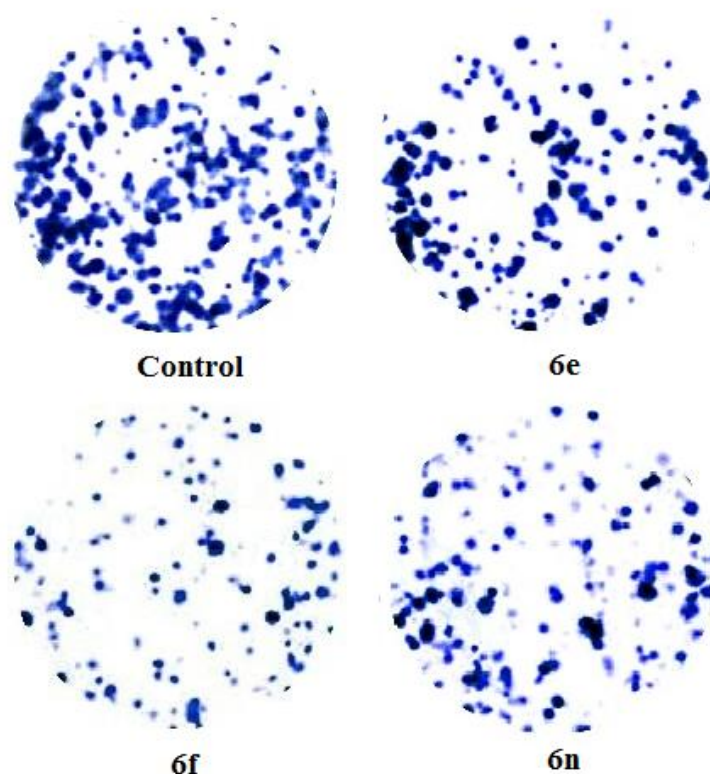


Figure 3: Colony formation inhibition assay of compounds **6e**, **6f** and **6n** in MCF-7 cancer cell line.

2.3.1.3 Hoechst staining

In order to determine apoptosis inducing potential of compounds, MCF-7 cells were incubated with IC_{50} concentration of compounds **6e**, **6f** and **6n** for a period of 24 h. Furthermore, the morphological changes were studied after Hoechst 33242 staining. Control cells treated with DMSO demonstrated uniformly dispersed chromatin with almost negligible apoptotic characteristics (**Figure 4**). On the contrary, 30-40% cells treated with compounds **6e**, **6f** and **6n** exhibited typical apoptotic characteristics, like condensation of chromatin (brightly stained cells) and advent of fragmented apoptotic nucleus (indicated by arrowheads). Amongst the tested compounds, compound **6f** was found to be most potent apoptosis inducer (45% apoptosis cells) compared to the other two compounds, *i.e.*, **6n** (28% apoptotic cells) and **6e** (35% apoptotic cells). The results demonstrated the apoptosis inducing potential of the compounds against MCF-7 cancer cell line.

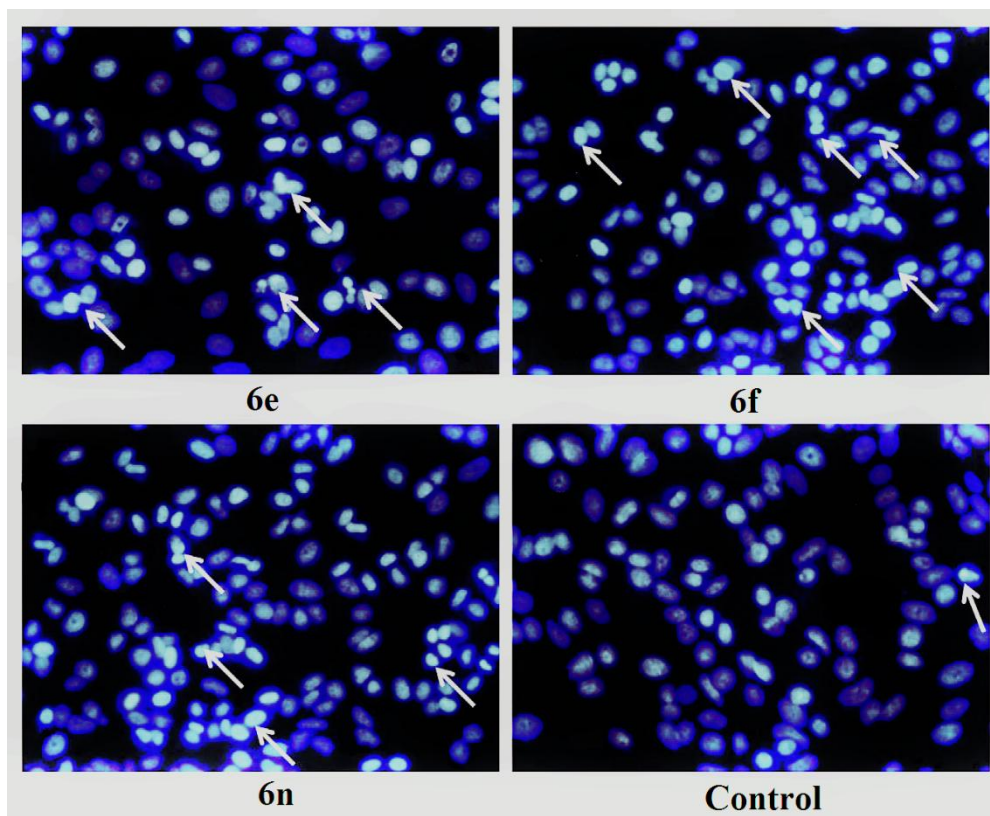


Figure 4: Hoechst staining of MCF-7 cells treated with compounds **6e**, **6f** and **6n**.

2.3.1.4 DNA fragmentation assay

The higher order chromatin structure of DNA is degraded by the activated nucleases into mono and oligo nucleosomal DNA-fragments during the apoptotic process. Therefore, a characteristic DNA ladder on agarose gel electrophoresis is formed as a result of loss of DNA content due to fragmentation of DNA [42]. Thus, in order to further confirm the apoptosis inducing effect of these compounds, DNA fragmentation assay was performed. MCF-7 cells were treated with the IC_{50} concentration of compounds **6e**, **6f** and **6n** for 24 h and chromosomal DNA was extracted. Agarose based gel electrophoresis was used to examine the apoptotic degradation of DNA. DNA from the cells treated by compounds exhibited a typical DNA smeared ladder pattern, an indicative of DNA fragmentation. In case of treatment with the synthesized compound **6f**, a typical DNA smeared ladder pattern was observed that clearly indicated fragmentation (**Figure 5**). DNA breaks at several positions across the chromosomal DNA resulted in smear of this type. Significantly intense smear was seen in DNA of cells treated with compounds **6f** and **6n**. However, moderate smear formation was seen in case of compound **6e**. DNA from control cells showed little or no signs of DNA

degradation. Results obtained using MCF-7 cells clearly indicate that compounds **6f** and **6n** are apoptosis inducing agents.

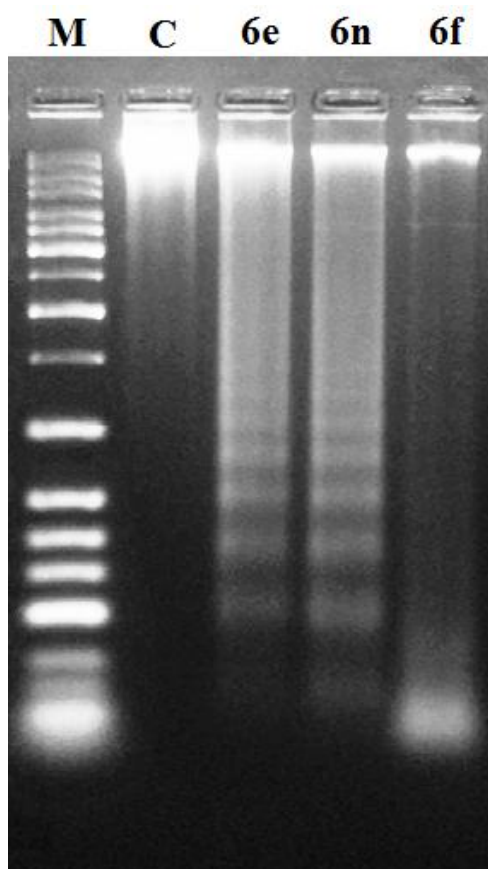


Figure 5: DNA ladder assay of compounds **6e**, **6f** and **6n** in MCF-7 cell line, **C** is Control (Untreated) and **M** is Molecular Weight Marker.

2.3.2 Anti-inflammatory

2.3.2.1 Protein Albumin Denaturation Assay

Protein (egg albumin) denaturation assay was used to evaluate the *in vitro* anti-inflammatory activity of three most active compounds **6e**, **6f** and **6n**. Diclofenac sodium was used as the standard drug for performing assay. All three of the compounds demonstrated significant anti-inflammatory activity with IC_{50} values of 60.56, 57.24 and 69.15 $\mu\text{g/ml}$ for compounds **6e**, **6f** and **6n** respectively (**Table 2**). However, the IC_{50} value for the standard, Diclofenac Sodium was found to be 54.65 $\mu\text{g/mL}$.

Table 2: Anti-inflammatory activity of compounds **6e**, **6f** and **6n** on the basis of protein albumin denaturation assay.

Comp.	% Inhibition				IC ₅₀ (µg/mL)
	25 (µg/mL)	50 (µg/mL)	100 (µg/mL)	200 (µg/mL)	
6e	04.99 ± 1.08	68.21 ± 0.67	84.60 ± 0.64	100 ± 0.00	60.56 ± 0.46
6f	0.820 ± 0.69	74.43 ± 0.53	88.68 ± 0.29	100 ± 0.00	57.24 ± 0.95
6n	19.51 ± 0.89	48.28 ± 0.59	74.01 ± 0.49	100 ± 0.00	69.15 ± 0.45
Diclofenac Sodium	7.47 ± 0.66	67.31 ± 0.43	92.62 ± 0.58	100 ± 0.00	54.65 ± 0.71

2.3.2.2 Red Blood Cell Membrane Stabilizing Assay

In vitro anti-inflammatory activity was also assessed by another method called to be as red blood cell membrane stabilizing assay. Consequently, the results thus obtained revealed that the molecules inhibited RBC haemolysis in a concentration dependent manner (**Table 3**). Aspirin was used as standard. All of the compounds displayed noteworthy anti-inflammatory potential with compound **6f** as the most promising one.

Table 3: Anti-inflammatory activity of compounds **6e**, **6f** and **6n** on the basis of red blood cell membrane stabilizing assay.

Compounds	Concentration (µg/mL)	% Protection
6e	100	40.25 ± 3.72
	200	70.24 ± 1.02
	500	94.67 ± 1.84
6f	100	51.06 ± 1.09
	200	74.25 ± 2.65
	500	97.25 ± 3.27
6n	100	46.24 ± 2.65
	200	68.41 ± 3.01
	500	90.48 ± 2.08
Aspirin	100	60.14 ± 1.65
	200	84.23 ± 2.95

2.4. Molecular Docking

In order to assess the mechanism of action of the synthesized novel anticancer derivatives, molecular docking studies were performed on different anticancer targets particularly, tubulin.

Table 4: Dock Score of Synthesized compounds **4a-4e** and **6a-6o** against tubulin protein (PDB ID: 3E22)

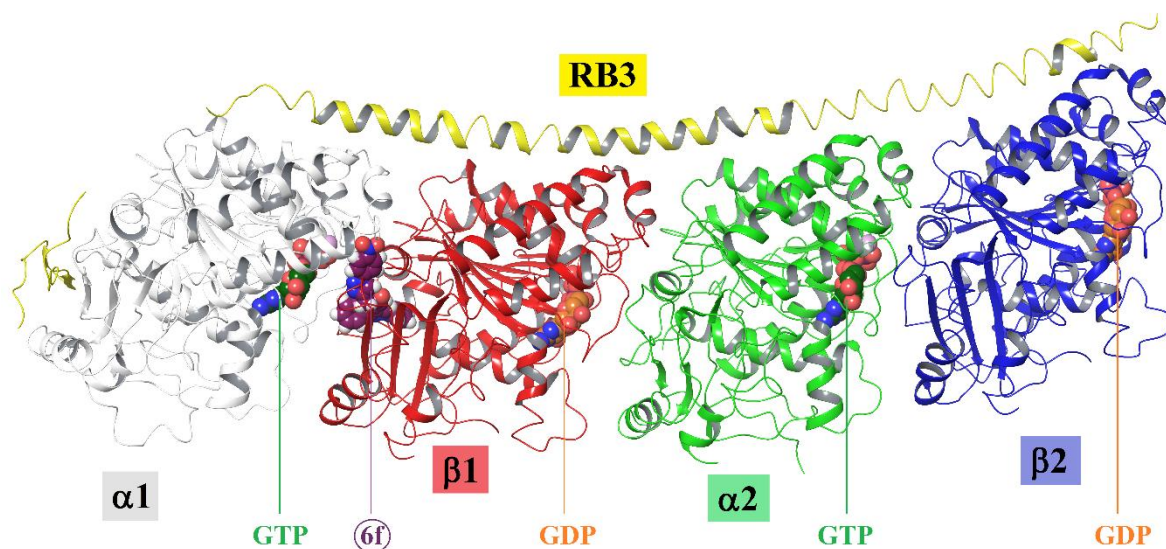
S. No.	Compd.	Dock Score	S. No.	Compd.	Dock Score	S. No.	Compd.	Dock Score
1.	4a	-6.611	8.	6c	-7.722	15.	6j	-7.192
2.	4b	-7.368	9.	6d	-7.703	16.	6k	-7.708
3.	4c	-6.290	10.	6e	-7.812	17.	6l	-5.442
4.	4d	-7.463	11.	6f	-8.047	18.	6m	-7.847
5.	4e	-6.116	12.	6g	-7.633	19.	6n	-7.737
6.	6a	-7.241	13.	6h	-7.474	20.	6o	-7.478
7.	6b	-7.377	14.	6i	-7.166	21.	Combretas tatin A4	-8.376

As a result of the molecular docking study, almost all of the compounds have shown noteworthy and remarkable interactions with the tubulin protein. Among all the compounds used in the study, triazoles (**6a-6o**) were found to have better interactions than the terminal alkyne containing propargyl derivatives (**4a-4e**). The dock scores ranged from -8.047 to -5.442 kCal/mol, with **6f** having the best score (-8.047) compared to the dock score of colchicine (-7.876). **Table 4** represents the Dock Score of different synthesized compounds against tubulin protein.

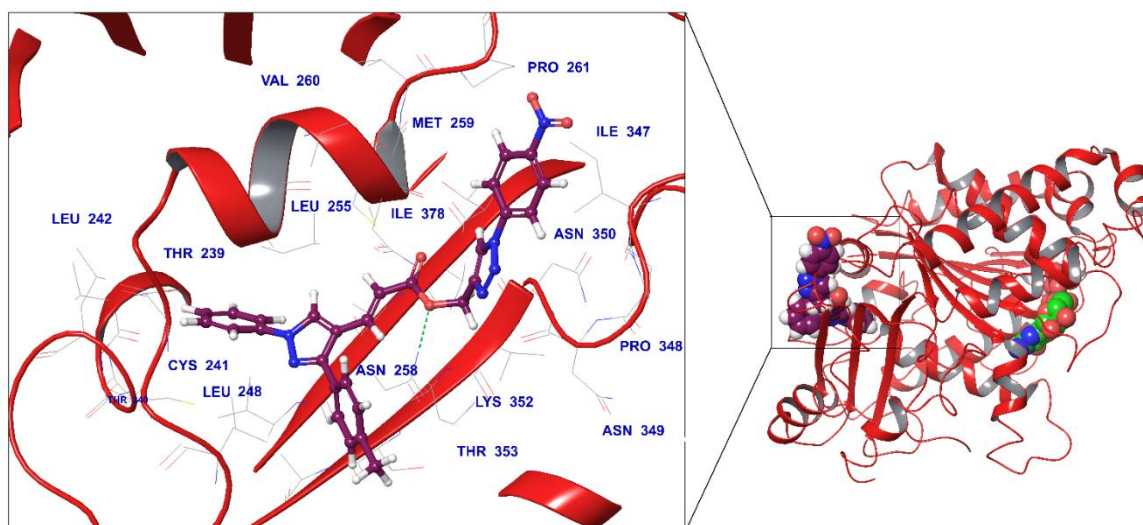
Cartoon representation of the overall structure of the complex formed between **6f** and tubulin is shown in **Figure 6a**. α -tubulin is shown in grey ($\alpha 1$) and green ($\alpha 2$), whereas β -tubulin is represented by red ($\beta 1$) and blue ($\beta 2$) color. RB3 Stathmin-like domain is shown in yellow color. GTP (green) and GDP (orange) molecules bound to the α -tubulin and β -tubulin are

displayed as CPK model. Also the most active compound (**6f**) can be seen bound to the β 1-tubulin in purple color CPK model form.

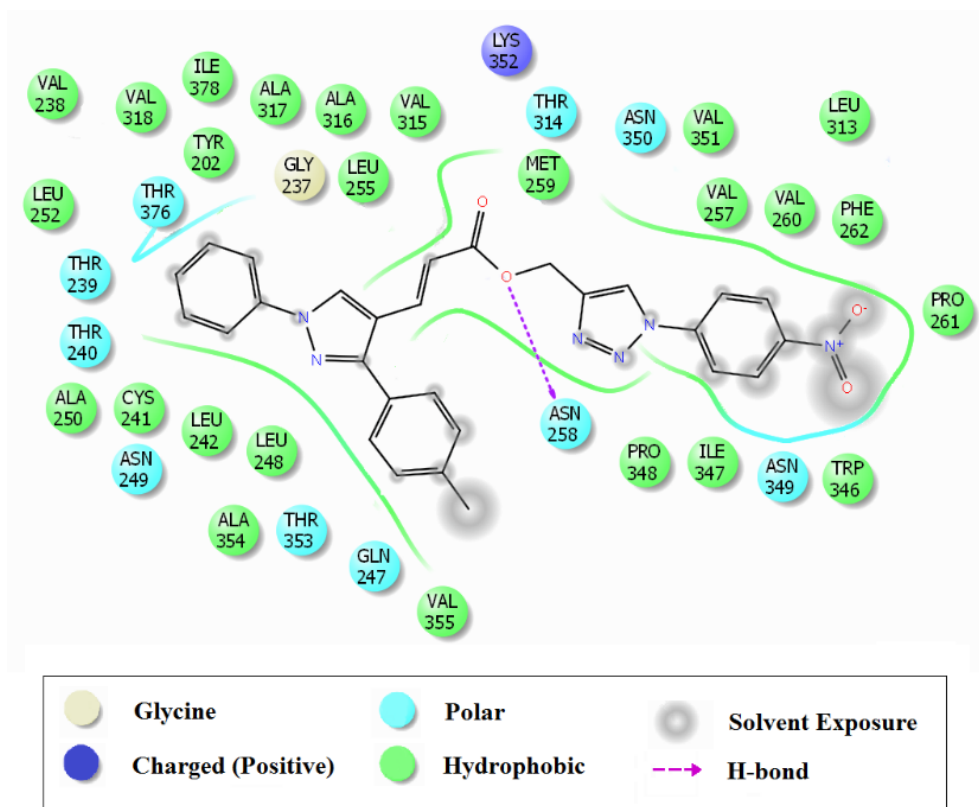
In order to have a deeper look into the molecular interactions of the most active compound **6f** and tubulin, the expanded image of the active site of β 1-tubulin bearing compound **6f** is displayed in **Figure 6b**. **Figure 6c** represent the Ligand Interaction Diagram (LID) depicting the molecular interactions of **6f** with tubulin protein. To understand the molecular interactions displayed in LID more evidently, legends for the same are also represented below the diagram.



6a



6b



6c

Figure 6: Docking Analysis for most active anticancer compound **6f** with tubulin (PDB ID: **3E22**). (a) Cartoon representation of the overall structure of the complex formed between **6f** and tubulin. (b) Dock pose of **6f** bound in the colchicine binding site of $\beta 2$ -tubulin. (c) 2-D Ligand Interaction Diagram of **6f** bound in the colchicine binding site of $\beta 2$ -tubulin.

From the results, it is quite evident that compound **6f** demonstrated interactions with a number of amino acid residues (**Figure 6c**). The bridging Oxygen of the ester group was found to form a hydrogen bond with the amino acid residue Asn 258. Compound **6f** interacted hydrophobically with numerous amino acid residues like Cys 241, Leu 242, Leu 248, Ala 250, Leu 252, Ala 316, Met 259, Pro 261, Trp 346, Ile 347, Val 355, *etc.* **6f** also exhibited significant polar interactions with amino acid residues like Thr 239, Gln 247, Asn 249, Asn 258, Thr 314, Asn 349, *etc.* The compound was found to have interaction with positively charged residue Lys 352 as well. Sufficient amount of solvent exposure is also found to be contributing towards good affinity of the molecule with the protein.

2.5 Structure-Activity Relationship

On comparing the *in vitro* anticancer results of the synthesized molecules (**4a-e**, **6a-o**), triazole containing compounds (**6a-o**) clearly demonstrated better results than the predecessor terminal alkyne containing acrylate derivatives (**4a-e**). The superior effect of di-phenyl pyrazole and triazole conjugates (**6a-o**) over di-phenyl pyrazole containing terminal alkynes (**4a-e**) may be attributed to the synergistic action of two pharmacophores when used in combination. Substitution of electron donating groups at –R position (over one of the phenyl ring of diphenyl pyrazole moiety) favored anticancer potential of the compounds as seen in compounds **6f**, **6e** and **6m** having methyl, methoxy and methoxy groups respectively. On the contrary, compounds bearing electron withdrawing groups like Chloro and Fluoro (**4c**, **4e**, **6j** and **6l**) at position –R were found to have diminished anticancer activity. Unsubstituted compounds (**6a**, **6b**, **6d**, **6g** and **6k**) were found to possess mediocre anticancer potential.

In case of substitutions over –X position (over phenyl ring directly attached to the triazole ring), the situation was found to be just opposite. Here, substitution of electron withdrawing groups resulted in boosting the anticancer potential. This is quite evident from compounds **6f** and **6n** (containing Nitro group), **6e** (containing Chloro group) and compounds **6k** and **6m** (containing 3-Chloro and 4-Fluoro substitutions). Whereas, compounds bearing electron donating groups like Methyl group (**6i** and **6l**) were found to possess poor anticancer potential.

3. Experimental

3.1 Chemistry

All the required chemicals and reagents used in the reactions were purchased from commercial vendors. These chemicals were not purified further. Aluminum backed silica plates (Merck, silica gel 60 F254) were used to perform Thin layer chromatography (TLC). Melting points were reported by using open capillaries and are uncorrected. Bruker alpha-T spectrophotometer was used to record Infra-red (IR) spectra. Bruker Avance-400 was used for recording Nuclear Magnetic Resonance (NMR) spectra. Frequencies of 400 and 100 MHz were used for recording ^1H and ^{13}C spectra respectively. CDCl_3 served as the solvent to dissolve triazole derivatives whereas Tetramethylsilane (TMS) was taken as an internal standard. Chemical shift values (δ) are reported in *parts per million (ppm)* whereas coupling constants (J) are reported in *Hertz (Hz)*. Xevo G2-XS QTOF, equipped with electrospray (ESI) ionization spray source was used to record high resolution mass spectra (HRMS). This

was operated in full scan positive mode. For a few compounds, mass spectra were recorded on Synapt mass spectrometer (UPLCMS/MS). Purity of certain compounds was determined by UPLC (WATERS INC.). Perkin-Elmer-240 was used for elemental analysis. Column chromatography was done wherever required using silica gel of 60-120 mm taking hexane and ethyl acetate in the ratio of 7 : 3 v/v respectively, as the solvent system.

3.1.1 Synthesis of 1,3-Diphenyl-1H-pyrazole-4-carbaldehyde (**2a-e**)

1,3-Diphenyl-1H-pyrazole-4-carbaldehydes (**2a-e**) were synthesized as per the method reported in literature [43, 44]. The aldehydes thus obtained were found to have spectral and other analytical data in agreement with the data reported in the literature.

3.1.2 Synthesis of 3-(1,3-diphenyl-1H-pyrazol-4-yl)acrylic acid derivatives (**3a-e**)

Synthesis of 3-(1,3-diphenyl-1H-pyrazol-4-yl)acrylic acid derivatives was carried out according to our previously reported method. Details for derivatives **3a-c** have already been published by our group [34]. Spectral details for newly synthesized derivatives **3d** and **3e** have been incorporated in the **Supplementary Information** section.

3.1.3 Synthesis of Prop-2-ynyl-3-(1,3-diphenylpyrazol-4-yl)prop-2-enoate (**4a-e**)

Pyrazole acids (1 mM) (**3a-e**) were dissolved in dried acetone, and fused potassium carbonate (4 mM) was added to it. The resulting mixture was then heated with stirring for 30 min. After that, propargyl bromide (1 mM) was added and stirring with heating was continued till the completion of reaction. Potassium carbonate was then filtered from the hot reaction mixture, and the filtrate was poured in ice cold water. The precipitate thus obtained was filtered, washed with water and dried. Spectral details for compounds **4a-e** are depicted in the **Supplementary Information** section.

3.1.4 Synthesis of aryl azides (**5a-h**)

Derivatives **5a-h** were synthesized in accordance with the reported methods [39].

3.1.5 Synthesis of (1-phenyl-1H-1,2,3-triazol-4-yl)methyl 3-(1,3-diphenyl-1H-pyrazol-4-yl)acrylate (**6a-6o**)

Scheme 1 represents the method adopted for the preparation of triazoles reported in this paper.

Different derivatives synthesized by this method are enlisted in **Table 5**. To a solution of terminal alkyne containing pyrazole acrylate derivatives (1 mM) (**4a-e**) and aryl azides (1.1 mM) (**5a-h**) in 1:1 mixture of water and DCM, sodium ascorbate (0.1 mM) and copper (II) sulphate (0.05 mM) were added sequentially. Reaction was stirred overnight at room temperature. Solvents were concentrated under vacuum and mixture was extracted with

DCM, dried and concentrated under vacuum. Further, all the compounds were purified by column chromatography using silica gel and solvent system hexane and ethyl acetate in the ratio 7 : 3 v/v , respectively.

(1-(2-nitrophenyl)-1H-1,2,3-triazol-4-yl)methyl 3-(1,3-diphenyl-1H-pyrazol-4-yl)acrylate
(**6a**)

Compound **6a** was synthesized by reaction of **4a** with **5a** as per the procedure given above. Appearance: White powder; Yield (%): 72; m.p. 176-178°C; ¹H NMR (400 MHz, CDCl₃): 5.43 (s, 2H, CH₂), 6.29 (d, 1H, *H*-α, *J*=16.0 Hz), 7.33 (t, 1H, *H*-4, *J*=7.2 Hz), 7.43-7.51 (m, 5H, *H*-3,5, 3',4',5'), 7.61-7.81 (m, 8H, *H*-2,6,2',6',4'',5'',6'',β), 7.97 (s, 1H, *H*-Triazole), 8.09 (d, 2H, *H*-3'', *J*=7.6 Hz), 8.25 (s, 1H, *H*-Pyrazole); IR (cm⁻¹): 1716 (C=O), 1523,1330 (NO₂), 1239 (C-O); Mass (*m/z*): 493.2 [M+H]⁺; Elemental analysis (%) of C₂₇H₂₀N₆O₄, calculated/found: C (65.85/65.86), H (4.09/4.12), N (17.06/17.08).

(1-(3-nitrophenyl)-1H-1,2,3-triazol-4-yl)methyl 3-(1,3-diphenyl-1H-pyrazol-4-yl)acrylate
(**6b**)

Compound **6b** was synthesized by reaction of **4a** with **5b** as per the procedure given above. Appearance: White powder; Yield (%): 70; m.p. 196-198°C; ¹H NMR (400 MHz, CDCl₃): 5.44 (s, 2H, CH₂), 6.29 (d, 1H, *H*-α, *J*=16.0 Hz), 7.33 (t, 2H, *H*-4, *J*=7.6 Hz), 7.42-7.51 (m, 5H, *H*-3,5,3',4',5'), 7.66 (d, 2H, *H*-2,6, *J*=8.4 Hz), 7.74-7.82 (m, 4H, *H*-2',6',5'',β), 8.17 (dd, 1H, *H*-6'', *J*=1.6 Hz), 8.20 (s, 1H, *H*-Triazole), 8.25 (s, 1H, *H*-Pyrazole), 8.31 (dd, 1H, *H*-4'', *J*= 8.8 & 1.6 Hz), 8.61 (t, 1H, *H*-2'', *J*=2 Hz); IR (cm⁻¹): 1719 (C=O), 1534, 1328 (NO₂), 1219 (C-O); Mass (*m/z*): 493.5 [M+H]⁺; Elemental analysis (%) of C₂₇H₂₀N₆O₄, calculated/found: C (65.85/65.84), H (4.09/4.08), N (17.06/17.08).

(1-(2-nitrophenyl)-1H-1,2,3-triazol-4-yl)methyl 3-(3-(4-chlorophenyl)-1-phenyl-1H-pyrazol-4-yl)acrylate (**6c**)

Compound **6c** was synthesized by reaction of **4e** with **5a** as per the procedure given above. Appearance: white powder; Yield (%): 66; m.p. 182-184°C; ¹H NMR (400 MHz, CDCl₃): 5.44 (s, 2H, CH₂), 6.30 (d, 1H, *H*-α, *J*= 16.0 Hz), 7.34 (t, 1H, *H*-4, *J*= 7.6 Hz), 7.45-7.52 (m, 4H, *H*-3,5,3',5'), 7.60-7.64 (m, 3H, *H*-2,6,4''), 7.72-7.76 (m, 4H, *H*-2',6',6'',β), 7.79 (t, 1H, *H*-5'', *J*= 8.8 Hz), 7.97 (s, 1H, *H*-Triazole), 8.10 (d, 1H, *H*-3'', *J*= 7.6 Hz), 8.24 (s, 1H, *H*-Pyrazole); IR (cm⁻¹): 1721 (C=O), 1535, 1336 (NO₂), 1267 (C-O); Mass (*m/z*): 527.7

$[M+H]^+$; Elemental analysis (%) of $C_{27}H_{19}ClN_6O_4$, calculated/found: C (61.54/61.52), H (3.63/3.64), N (15.95/15.96).

(1-(3-chlorophenyl)-1H-1,2,3-triazol-4-yl)methyl 3-(1,3-diphenyl-1H-pyrazol-4-yl)acrylate (6d)

Compound **6d** was synthesized by reaction of **4a** with **5c** as per the procedure given above. Appearance: White powder; Yield (%): 69; m.p. 102-104°C; 1H NMR (400 MHz, $CDCl_3$): 5.44 (s, 2H, CH_2), 6.30 (d, 1H, $H-\alpha$, $J=16.0$ Hz), 7.33 (t, 1H, $H-4$, $J=7.6$ Hz), 7.41-7.51 (m, 7H, $H-3,5,3',4',5',2'',4''$), 7.58-7.64 (m, 2H, $H-5'',6''$), 7.66 (d, 2H, $H-2,6$, $J=6.8$ Hz), 7.75 (d, 2H, $H-2',6'$, $J=7.2$ Hz), 7.77 (d, 1H, $H-\beta$, $J=15.6$ Hz), 8.09 (s, 1H, H -Triazole), 8.24 (s, 1H, H -Pyrazole); ^{13}C NMR (100 MHz, $CDCl_3$): (57.48, 116.61, 117.50, 119.39, 125.98, 126.55, 127.29, 127.81, 127.96, 128.60, 128.72, 128.81, 129.59, 130.81, 130.89, 132.13, 134.75, 136.21, 139.39, 142.90, 153.46, 166.84); IR (cm^{-1}): 1714 (C=O), 1265 (C-O); Mass (m/z): 482.3 $[M+H]^+$; Elemental analysis (%) of $C_{27}H_{20}ClN_5O_2$, calculated/found: C (67.29/67.30), H(4.18/4.15), N(14.53/14.55).

(1-(3-chlorophenyl)-1H-1,2,3-triazol-4-yl)methyl 3-(3-(4-methoxyphenyl)-1-phenyl-1H-pyrazol-4-yl)acrylate (6e)

Compound **6e** was synthesized by reaction of **4d** with **5c** as per the procedure given above. Appearance: White powder; Yield (%): 74; m.p. 88-90°C; 1H NMR (400 MHz, $CDCl_3$): 3.87 (s, 3H, OCH_3), 5.44 (s, 2H, CH_2), 6.29 (d, 1H, $H-\alpha$, $J=16.0$ Hz), 7.00 (d, 2H, $H-3',5'$, $J=8.4$ Hz), 7.32 (t, 1H, $H-4$, $J=7.2$ Hz), 7.45-7.52 (m, 4H, $H-3,5,2'',4''$), 7.59-7.64 (m, 4H, $H-2,6,5'',6''$), 7.74 (d, 2H, $H-2',6'$, $J=8.0$ Hz), 7.76 (d, 1H, $H-\beta$, $J=16.0$ Hz), 8.10 (s, 1H, H -Triazole), 8.22 (s, 1H, H -Pyrazole); IR (cm^{-1}): 1722 (C=O), 1263 (C-O); Mass (m/z): 512.6 $[M+H]^+$; Elemental analysis (%) of $C_{28}H_{22}ClN_5O_3$, calculated/found: C (65.69/65.66), H (4.33/4.35), N (13.68/13.69).

(1-(4-nitrophenyl)-1H-1,2,3-triazol-4-yl)methyl 3-(1-phenyl-3-(p-tolyl)-1H-pyrazol-4-yl)acrylate (6f)

Compound **6f** was synthesized by reaction of **4b** with **5d** as per the procedure given above. Appearance: White powder; Yield (%): 75; m.p. 194-196°C; 1H NMR (400 MHz, $CDCl_3$): 2.42 (s, 3H, CH_3), 5.43 (s, 2H, CH_2), 6.28 (d, 1H, $H-\alpha$, $J=16.0$ Hz), 7.34 (t, 1H, $H-4$, $J=7.2$ Hz), 7.44-7.52 (m, 4H, $H-3,5,3',5'$), 7.65 (d, 2H, $H-2,6$, $J=6.8$ Hz), 7.75 (d, 2H, $H-2',6'$, $J=$

8.0 Hz), 7.80 (d, 1H, $H-\beta$, $J= 16.0$ Hz), 7.97 (d, 2H, $H-2'',6''$, $J= 9.2$ Hz), 8.20 (s, 1H, H -Triazole), 8.24 (s, 1H, H -Pyrazole), 8.41 (d, 2H, $H-3'',5''$, $J= 9.2$ Hz); IR (cm^{-1}): 1727 (C=O), 1540, 1342 (NO_2), 1252 (C-O); Mass (m/z): 507.2 $[\text{M}+\text{H}]^+$; Elemental analysis (%) of $\text{C}_{28}\text{H}_{22}\text{N}_6\text{O}_4$, calculated/found: C (66.40/66.43), H (4.38/4.36), N (16.59/16.60).

(1-(4-fluorophenyl)-1H-1,2,3-triazol-4-yl)methyl 3-(1,3-diphenyl-1H-pyrazol-4-yl)acrylate (**6g**)

Compound **6g** was synthesized by reaction of **4a** with **5e** as per the procedure given above. Appearance: White powder; Yield (%): 67; m.p. 150-152°C; ^1H NMR (400 MHz, CDCl_3): 5.41 (s, 2H, CH_2), 6.28 (d, 1H, $H-\alpha$, $J=16.0$ Hz), 7.20 (t, 2H, $H-3'',5''$, $J= 8.8$ Hz), 7.33 (t, 1H, 4, $J=7.2$ Hz), 7.42-7.52 (m, 5H, $H-3,5,3',4',5'$), 7.66 (d, 2H, $H-2,6$, $J= 6.8$ Hz), 7.70-7.73 (m, 2H, $H-2'',6''$), 7.75 (d, 2H, $H-2',6'$, $J= 6.4$ Hz), 7.77 (d, 1H, $H-\beta$, $J= 15.6$ Hz), 8.04 (s, 1H, H -Triazole), 8.24 (s, 1H, H -Pyrazole); ^{13}C NMR (100 MHz, CDCl_3): (57.47, 116.49, 116.67, 116.90, 117.45, 119.40, 122.43, 122.59, 122.68, 126.55, 127.33, 128.73, 128.82, 129.60, 132.13, 136.32, 139.38, 143.95, 153.48, 166.93); IR (cm^{-1}): 1727 (C=O), 1259 (C-O); HRMS m/z measured for $\text{C}_{27}\text{H}_{20}\text{FN}_5\text{O}_2$ $[\text{M}+\text{H}]^+$ 466.1699, m/z calculated $[\text{M}+\text{H}]^+$ 466.1679; UPLC: 99.92% purity; Elemental analysis (%) of $\text{C}_{27}\text{H}_{20}\text{FN}_5\text{O}_2$, calculated/found: C (69.67/69.65), H(4.33/4.34), N(15.05/15.07).

(1-(p-tolyl)-1H-1,2,3-triazol-4-yl)methyl 3-(3-(4-methoxyphenyl)-1-phenyl-1H-pyrazol-4-yl)acrylate (**6h**)

Compound **6h** was synthesized by reaction of **4d** with **5f** as per the procedure given above. Appearance: White powder; Yield (%): 68; m.p. 126-128°C; ^1H NMR (400 MHz, CDCl_3): 2.43 (s, 3H, CH_3), 3.87 (s, 3H, OCH_3), 5.41 (s, 2H, CH_2), 6.27 (d, 1H, $H-\alpha$, $J=16.0$ Hz), 7.01 (d, 2H, $H-3',5'$, $J= 8.8$ Hz), 7.31-7.35 (m, 3H, $H-4,3'',5''$), 7.46 (t, 2H, $H-3,5$, $J= 8.0$ Hz), 7.59-7.62 (m, 4H, $H-2,6,2'',6''$), 7.74 (d, 2H, $H-2',6'$, $J= 8.0$ Hz), 7.75 (d, 1H, $H-\beta$, $J= 15.6$ Hz), 8.04 (s, 1H, H -Triazole), 8.21 (s, 1H, H -Pyrazole); ^{13}C NMR (100 MHz, CDCl_3): (21.13, 55.39, 57.55, 114.09, 114.28, 116.33, 117.30, 119.34, 119.58, 120.54, 120.59, 122.21, 126.49, 127.19, 129.44, 129.57, 129.97, 130.28, 130.59, 134.64, 136.40, 139.07, 139.42, 143.66, 153.29, 160.07, 166.98); IR (cm^{-1}): 1728 (C=O), 1258 (C-O); HRMS m/z measured for $\text{C}_{29}\text{H}_{25}\text{FN}_5\text{O}_3$ $[\text{M}+\text{H}]^+$ 492.2047, m/z calculated $[\text{M}+\text{H}]^+$ 492.2036; UPLC: 99.83% purity; Elemental analysis (%) of $\text{C}_{29}\text{H}_{25}\text{N}_5\text{O}_3$, calculated/found: C (70.86/70.85), H(5.13/5.11), N(14.25/14.27).

(1-(p-tolyl)-1H-1,2,3-triazol-4-yl)methyl 3-(1,3-diphenyl-1H-pyrazol-4-yl)acrylate (6i)

Compound **6i** was synthesized by reaction of **4a** with **5f** as per the procedure given above. Appearance: White powder; Yield (%): 66; m.p. 118-120°C; ¹H NMR (400 MHz, CDCl₃): 2.42 (s, 3H, CH₃), 5.41 (s, 2H, CH₂), 6.28 (d, 1H, *H*-α, *J*=16.0 Hz), 7.31-7.36 (m, 3H, *H*-4,3'',5''), 7.43-7.51 (m, 5H, *H*-3,5,3',4',5'), 7.59 (d, 2H, *H*-2,6, *J*= 8.4 Hz), 7.65 (d, 2H, *H*-2'',6'', *J*= 8.4 Hz), 7.75 (d, 2H, *H*-2',6', *J*= 7.6 Hz), 7.76 (d, 1H, *H*-β, *J*= 16.0 Hz), 8.04 (s, 1H, *H*-Triazole), 8.24 (s, 1H, *H*-Pyrazole); ¹³C NMR (100 MHz, CDCl₃): (21.23, 57.57, 116.61, 117.49, 119.40, 120.54, 122.21, 126.55, 127.30, 128.81, 129.59, 130.27, 132.13, 134.63, 136.21, 139.39, 143.64, 153.47, 166.92); IR (cm⁻¹): 1719 (C=O), 1270 (C-O); Mass (*m/z*): 462.3 [M+H]⁺; Elemental analysis (%) of C₂₈H₂₃N₅O₂, calculated/found: C (72.87/72.89), H(5.02/5.00), N(15.17/15.16).

(1-(3-nitrophenyl)-1H-1,2,3-triazol-4-yl)methyl 3-(3-(4-fluorophenyl)-1-phenyl-1H-pyrazol-4-yl)acrylate (6j)

Compound **6j** was synthesized by reaction of **4c** with **5b** as per the procedure given above. Appearance: White powder; Yield (%): 68; m.p. 168-170°C; ¹H NMR (400 MHz, CDCl₃): 5.44 (s, 2H, CH₂), 6.28 (d, 1H, *H*-α, *J*=16.0 Hz), 7.16 (t, 2H, *H*-3',5', *J*=8.8 Hz), 7.34 (t, 1H, *H*-4, *J*=7.6 Hz), 7.47 (t, 2H, *H*-3,5), 7.63-7.66 (m, 2H, *H*-2,6), 7.73-7.78 (m, 4H, *H*-2',6',5'',β), 8.18 (dd, 1H, *H*-6'', *J*= 6.8 Hz & 1.6 Hz), 8.20 (s, 1H, *H*-Triazole), 8.24 (s, 1H, *H*-Pyrazole), 8.31 (dd, 1H, *H*-4'', *J*= 7.6 Hz & *J*= 1.6 Hz), 8.61 (t, 1H, *H*-2'', *J*= 2.0 Hz); IR (cm⁻¹): 1714 (C=O), 1526, 1329 (NO₂), 1219 (C-O); Mass (*m/z*): 511.6 [M+H]⁺; Elemental analysis (%) of C₂₇H₁₉FN₆O₄, calculated/found: C (63.53/63.55), H(3.75/3.77), N(16.46/16.43).

(1-(3-chloro-4-fluorophenyl)-1H-1,2,3-triazol-4-yl)methyl 3-(1,3-diphenyl-1H-pyrazol-4-yl)acrylate (6k)

Compound **6k** was synthesized by reaction of **4a** with **5g** as per the procedure given above. Appearance: Brick red powder; Yield (%): 74; m.p. 160- 162°C; ¹H NMR (400 MHz, CDCl₃): 5.41 (s, 2H, CH₂), 6.28 (d, 1H, *H*-α, *J*=16.0 Hz), 7.29-7.37 (m, 2H, *H*-4,5''), 7.44-7.51 (m, 5H, *H*-3,5,3',4',5'), 7.61-7.67 (m, 3H, *H*-2,6,2''), 7.75 (d, 2H, *H*-2',6', *J*= 6.8 Hz), 7.77 (d, 1H, *H*-β, *J*= 16.0 Hz), 7.84 (dd, 1H, *H*-6'', *J*= 6.4 Hz & 2.4 Hz), 8.05 (s, 1H, *H*-Triazole), 8.24 (s, 1H, *H*-Pyrazole); IR (cm⁻¹): 1720 (C=O), 1230 (C-O); Mass (*m/z*): 500.1

[M+H]⁺; Elemental analysis (%) of C₂₇H₁₉ClFN₅O₂, calculated/found: C (64.87/64.86), H (3.83/3.85), N(14.01/14.04).

(1-(o-tolyl)-1H-1,2,3-triazol-4-yl)methyl 3-(3-(4-chlorophenyl)-1-phenyl-1H-pyrazol-4-yl)acrylate (6l)

Compound **6l** was synthesized by reaction of **4e** with **5h** as per the procedure given above. Appearance: White powder; Yield (%): 76; m.p. 172-174°C; ¹H NMR (400 MHz, CDCl₃): 2.18 (s, 3H, CH₃), 5.30 (s, 2H, CH₂), 6.55 (d, 1H, *H*-α, *J*= 16.0 Hz), 6.90 (d, 1H, *H*-3'', *J*= 8.4 Hz), 7.36 (t, 1H, *H*-4, *J*=7.2 Hz), 7.46 (dd, 1H, *H*-5'', *J*=8 Hz & 2.4 Hz), 7.53-7.66 (m, 9H, *H*-2,3,5, 6,3',5',4'',6'',β), 7.88 (d, 2H, *H*-2',6', *J*=8.8 Hz), 8.66 (s, 1H, *H*-Triazole), 9.25 (s, 1H, *H*-Pyrazole); IR (cm⁻¹): 1725 (C=O), 1238 (C-O); Mass (*m/z*): 496.4 [M+H]⁺; Elemental analysis (%) of C₂₈H₂₂ClN₅O₂, calculated/found: C (67.81/67.82), H (4.47/4.45), N (14.12/14.13).

(1-(3-chloro-4-fluorophenyl)-1H-1,2,3-triazol-4-yl)methyl 3-(3-(4-methoxyphenyl)-1-phenyl-1H-pyrazol-4-yl)acrylate (6m)

Compound **6m** was synthesized by reaction of **4d** with **5g** as per the procedure given above. Appearance: White powder; Yield (%): 72; m.p. 170-172°C; ¹H NMR (400 MHz, CDCl₃): 3.88 (s, 3H, OCH₃), 5.40 (s, 2H, CH₂), 6.26 (s, 1H, *H*-α, *J*= 16.0 Hz), 7.00 (d, 2H, *H*-3',5', *J*= 8.8 Hz), 7.15 (d, 1H, *H*-5'', *J*=8.8 Hz), 7.32 (t, 1H, *H*-4, *J*=6.8 Hz), 7.46-7.60 (m, 6H, *H*-2,3,5,6,2',6'), 7.74-7.79 (m, 3H, *H*-2',6',β), 8.00 (s, 1H, *H*-Triazole), 8.21 (s, 1H, *H*-Pyrazole); IR (cm⁻¹): 1721 (C=O), 1248 (C-O); Mass (*m/z*): 530.1 [M+H]⁺; Elemental analysis (%) of C₂₈H₂₁ClFN₅O₃, calculated/found: C (63.46/63.44), H (3.99/4.01), N (13.22/13.24).

(1-(4-nitrophenyl)-1H-1,2,3-triazol-4-yl)methyl 3-(1,3-diphenyl-1H-pyrazol-4-yl)acrylate (6n)

Compound **6n** was synthesized by reaction of **4a** with **5d** as per the procedure given above. Appearance: White powder; Yield(%): 80; m.p. 208-210°C; ¹H NMR (400 MHz, CDCl₃): 5.43 (s, 2H, CH₂), 6.28 (d, 1H, *H*-α, *J*=16.0 Hz), 7.33 (t, 1H, *H*-4, *J*=7.6 Hz), 7.42-7.51 (m, 5H, *H*-3,5,3',4',5'), 7.65 (d, 2H, *H*-2,6, *J*=7.2 Hz), 7.75 (d, 2H, *H*-2',6', *J*=8.4 Hz), 7.77 (d, 1H, *H*-β, *J*=15.6 Hz), 7.97 (d, 2H, *H*-2'',6'', *J*=8.8 Hz), 8.20 (s, 1H, *H*-Triazole), 8.24 (s, 1H, *H*-Pyrazole), 8.41 (d, 2H, *H*-3'',5'', *J*=9.2 Hz); IR (cm⁻¹): 1726 (C=O), 1545, 1330 (NO₂), 1236 (C-O); HRMS *m/z* measured for C₂₇H₂₀FN₆O₄ [M+H]⁺ 493.1602, *m/z* calculated

$[M+H]^+$ 493.1624; Elemental analysis (%) of $C_{27}H_{20}N_6O_4$, calculated/found: C (65.85/65.83), H(4.09/4.11), N(17.06/17.07).

(1-(p-tolyl)-1H-1,2,3-triazol-4-yl)methyl 3-(1-phenyl-3-(p-tolyl)-1H-pyrazol-4-yl)acrylate
(60)

Compound **60** was synthesized by reaction of **4b** with **5f** as per the procedure given above. Appearance: Brick red powder; Yield(%): 68; m.p. 128-130°C; 1H NMR (400 MHz, $CDCl_3$): 2.42 (s, 6H, $2 \times CH_3$), 5.41 (s, 2H, CH_2), 6.27 (d, 1H, $H-\alpha$, $J=16.0$ Hz), 7.28-7.36 (m, 5H, $H-4,3',5',3'',5''$), 7.46 (t, 2H, $H-3,5$, $J=7.6$ Hz), 7.54 (d, 2H, $H-2'',6''$, $J=8.4$ Hz), 7.60 (d, 2H, $H-2,6$, $J=8.0$ Hz), 7.74 (d, 2H, $H-2',6'$, $J=7.6$ Hz), 7.76 (d, 1H, $H-\beta$, $J=14.4$ Hz), 8.04 (s, 1H, H -Triazole), 8.22 (s, 1H, H -Pyrazole); ^{13}C NMR (100 MHz, $CDCl_3$): (21.13, 21.37, 57.54, 116.40, 117.43, 119.37, 119.61, 120.55, 122.21, 126.50, 127.21, 128.59, 129.24, 129.32, 129.51, 129.56, 130.27, 134.64, 136.38, 138.62, 139.07, 139.43, 143.67, 153.54, 166.95); IR (cm^{-1}): 1718 (C=O), 1251 (C-O); Mass (m/z): 476.3 $[M+H]^+$; Elemental analysis (%) of $C_{29}H_{25}N_5O_2$, calculated/found: C (73.25/73.27), H (5.30/5.27), N (14.73/14.75).

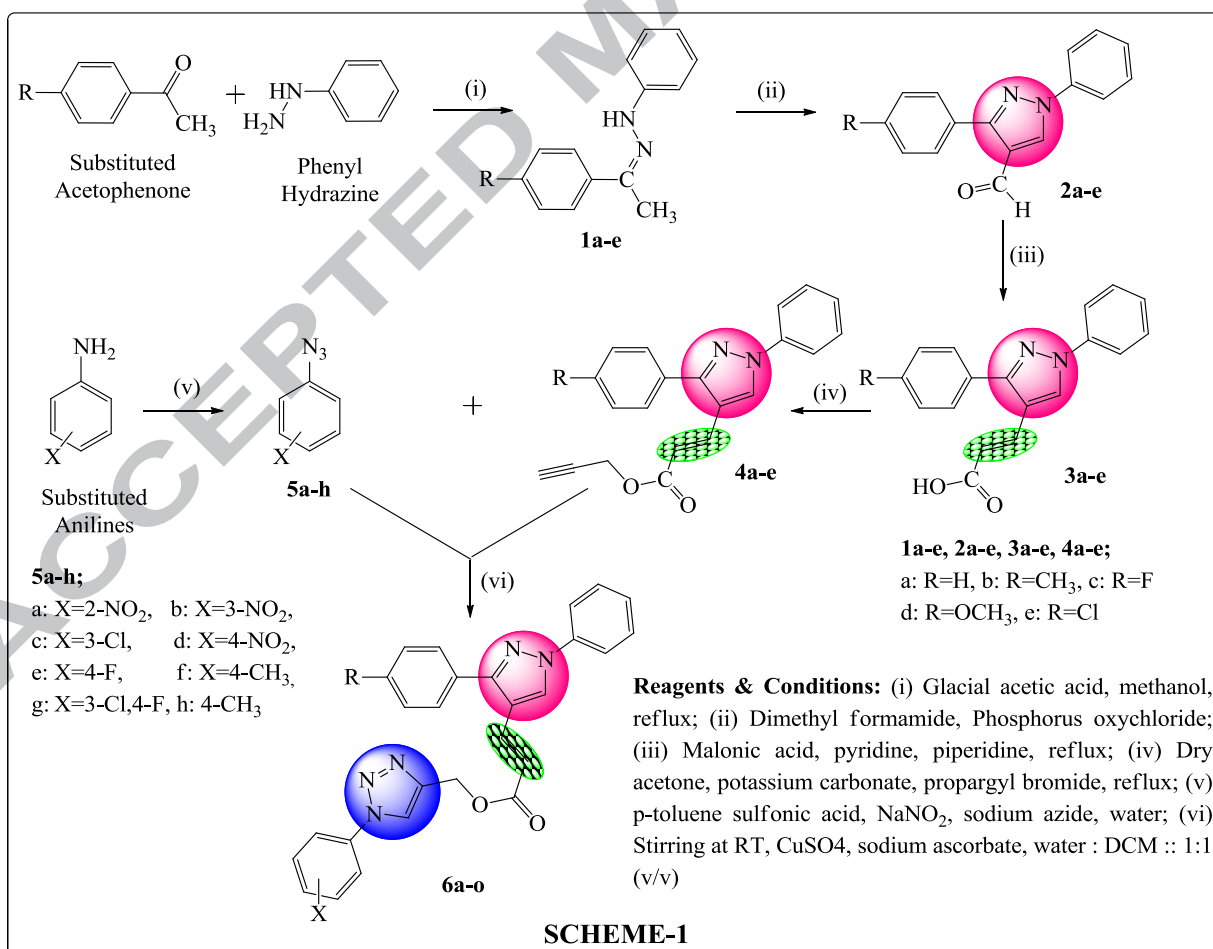


Table 5: List of Derivatives Synthesized Under Scheme 1

Compound	R	X	Compound	R	X	Compound	R	X
6a	-H	2-NO ₂	6f	-CH ₃	4-NO ₂	6k	-H	3-Cl,4-F
6b	-H	3-NO ₂	6g	-H	4-F	6l	-Cl	2-CH ₃
6c	-Cl	2-NO ₂	6h	-OCH ₃	4-CH ₃	6m	-OCH ₃	3-Cl,4-F
6d	-H	3-Cl	6i	-H	4-CH ₃	6n	-H	4-NO ₂
6e	-OCH ₃	3-Cl	6j	-F	3-NO ₂	6o	-CH ₃	4-CH ₃

3.2 Biological Activity

3.2.1 Anticancer

3.2.1.1. Sulforhodamine B Assay

For evaluating anticancer potential of the synthesized compounds, certain human cancer cell lines- MCF-7 (breast), A549 (Lung) and HCT-116 and HT-29 (Colon) were obtained from National Cancer Institute (NCI). Growth of all these cell lines was achieved in tissue culture flasks in complete medium (RPMI-1640) supplemented with 100 µg/mL streptomycin, 10% fetal bovine serum and 100 units/mL penicillin in carbon dioxide incubator (New Brunswick, Galaxy 170R, Eppendorf) at 5% CO₂, 37°C and 98% RH.

96-well cell culture plates were employed for performing sulforhodamine B (SRB) assay. To each well, 100 µL of the cell suspension of desired density was added and incubated (5% CO₂, 37°C, 90 % RH) for 24 h. Following incubation for the stipulated time period, 100 µL of the test samples were added into the wells supplemented with cells. These culture plates were again incubated for a period of 48 h. Depending on the requirements, controls, blanks and positive controls were also included in every experiment. Following incubation for the stipulated period, cells were fixed using 50 µL of ice-cold TCA (50%) for 1 h at a temperature of 4°C. Further, plates were washed using distilled water and then air dried. Following complete drying, addition of SRB dye (100 µL) was made to every well and was then allowed to stain for 30 min at room temperature. In order to remove excessive dye, plates were washed with 1 % acetic acid for five times. These plates were then air dried. Solubilisation of adsorbed dye was done by addition of 100 µL of 10 mM Tris Buffer (pH 10.5) to each well. Following this, these plates were shaken on shaker platform for a duration

of 5 min. 96-well ELISA plate reader (Molecular Devices, Sunnydale, USA) was used for reading these plates. Every sample was run in triplicate fashion. Mean value of these readings was taken for getting the results. Concentration of DMSO in cultures was kept < 1% [45].

$$\% \text{ Cell Viability} = 100 \times (T - T_0) / (C - T_0)$$

$$\% \text{ Growth inhibition} = 100 - \% \text{ Cell viability.}$$

T: Absorbance of Test sample

T₀: Absorbance of Blank

C: Absorbance of Control

3.2.1.2 Colony formation inhibition assay

Plating of MCF-7 cells at a density of 500 cells/well was done into 6-well culture plates. An adherence period of 24 h was given before treatment. Incubation of the cells was done with culture medium containing compounds **6e**, **6f** and **6n** at IC₅₀ concentration. Following a period of 24h, medium was replaced with fresh medium and further, the cells were incubated for a period of 14 days. Washing of cells was then done using 150 mM PBS (pH 7.4) followed by fixing using 4% paraformaldehyde, staining with 0.5% methylene blue in 10% ethanol for 30 min and finally rinsing with distilled water for removing excess dye. Plates were then photographed using a digital camera.

3.2.1.3 Hoechst staining

For Hoechst staining, seeding of MCF-7 cells was done at a density of 5×10^4 cells/well using 12 well tissue culture plates. Incubation period was set to 24 h. After this, media containing IC₅₀ concentrations of the compounds **6e**, **6f** and **6n** was used to replace the culture medium. It was then incubated for 24 h. Following this, 4% para formaldehyde was used to fix the cells. Further, Hoechst 33242 (5 µg/mL) was used for 30 min at room temp to stain the cells. Washing of cells was then done using 150 mM PBS (pH 7.4) to remove excess dye. Fluorescence microscopy (filters, excitation 350 nm and emissions 460 nm) was used to capture the images of stained nuclei from each well from randomly selected fields to find apoptotic cells.

3.2.1.4 DNA fragmentation assay

In six-well plates, MCF-7 cells were seeded (1×10^6 cells/well) and then incubated for 24 h. Following this, cells were subjected to the treatment with IC_{50} concentration of compounds **6e**, **6f** and **6n** for 24 h. Trypsinisation was used to harvest the cells and centrifugation at 2500 rpm for 5 min at 4°C was done. Then the pellet was collected and washing was done using phosphate buffered saline (150 mM PBS; pH 7.4). 400 µg/mL DNase free RNase A containing 250 µL of lysis buffer (100 mM NaCl, 5 mM EDTA, 10 mM Tris HCl pH 8.0, 0.25% SDS) was added and incubated for 90 min at 37°C. This was followed by incubation with proteinase K (200 µg/mL) for 1 h at 50°C. The samples were then centrifuged for 5 min at 3000 rpm at 4°C and the supernatant was then collected. 65 µL of ammonium acetate (10M) and ice cold ethanol (500 µL) was added and mixed well. The samples were then incubated for 1 h at -80°C and were further subjected to centrifugation at 12000 rpm at 4°C for 20 min. Washing of the pellet with 80% ethanol was done followed by air-drying for 10 min at room temperature. After drying, the pellet was dissolved in 50 µL of TBE buffer. Finally, 1.5% agarose gel electrophoresis in TBE Buffer was used to visualize DNA laddering after staining with ethidium bromide, which was followed by photography using digital camera.

3.2.2 Anti-inflammatory

3.2.2.1 Protein Albumin Denaturation Assay

In vitro protein denaturation method was adopted for determining anti-inflammatory potential of the most active anticancer compounds **6e**, **6f** and **6n**. Method described by Mizushima and Kobayashi was used for *in vitro* assessment. Bovine serum albumin and egg albumin proteins were dissolved in 50 mM sodium phosphate buffer (pH 6.4) at a concentration of 1%. The reaction mixture comprised test sample (0.1 mL, 1mg/mL) and 0.2 mL albumin protein. Final volume of the reaction mixture was made to 5 mL using buffer. Incubation of the reaction mixture was done at 37°C for a period of 20 min. This mixture was then heated to 95°C for 20 min. Following this, the reaction mixture was brought to room temperature and turbidity was measured using UV-visible spectrophotometer at 660 nm. The entire experiment was done in triplicate and average values were calculated. Finally, percentage inhibition of protein denaturation was calculated using the following formula.

$$\text{Percent Inhibition} = [(\text{Abs. Control} - \text{Abs. Sample})/\text{Abs. Control}] \times 100$$

Here:

Abs. Control: Absorbance of Control

Abs. Sample: Absorbance of Test sample

3.2.2.2 Red Blood Cell Membrane Stabilizing Assay

In this method, 5 mL of blood was collected from healthy adult rat and mixed with 5.0 mL of Alsever solution. Alsever solution comprised of 2.0% dextrose, 0.8% sodium citrate, 0.5% citric acid and 0.42% NaCl in water. The complete mixture was then centrifuged at 300 rpm. Packed cells were washed with isosaline (0.85%, pH 7.2) thrice for removal of cell debris. Assay mixture comprised of different concentrations of test sample (100, 200 and 500 µg/mL), 1.0 mL phosphate buffer (0.15 M, pH 7.4), 2.0 mL hyposaline (36%) and 0.5 mL red blood cell suspension. The complete mixture was incubated at 37°C for 30 min. followed by centrifugation at 3000 rpm for 20 min. Spectrophotometer was used for determining haemoglobin content of the supernatant at 560 nm. Aspirin (100 and 200 µg/mL) served as the standard. Percentage of RBC membrane stabilization was determined using formula.

$$\% \text{ Protection: } [(OD_1 - OD_2) / OD_1] \times 100$$

Here:

OD₁: Optical density of test sample

OD₂: Optical density of control

3.3 Molecular Docking

Catalytic domain of tubulin with PDB ID 3E22 was downloaded from RCSB protein data bank. [46]. Protein preparation was done using protein preparation wizard [47], a module of Schrödinger 2016-1. Water molecules without 3H bonds were removed. Following this, addition of hydrogen bonds corresponding to pH 7 was made considering proper ionization states for both basic and acidic amino acid residues. The energy of the crystal structure was minimized by using force field, OPLS_2005. Further, colchicine bound to tubulin protein was selected as its center for generating the grid box at active site's centroid. Around the centroid, a radius of 16Å was selected in order to define the active site.

Finally, docking of all low energy conformations into the catalytic domain of protein was done using Grid based Ligand Docking with Energetics (Glide v7.0, Schrödinger 2016-1) in standard precision (SP) mode in the absence of any constraints.

4. Conclusion

In the present study, synthesis and anticancer evaluation of series of 1,2,3-triazole linked 3-(1,3-diphenyl-1*H*-pyrazol-4-yl)acrylates have been carried out. Amongst all the synthesized compounds, compound **6f** showed most promising anticancer effects with IC₅₀ value of 1.962, 3.597, 1.764 and 4.496 μ M against A549, HCT-116, MCF-7 and HT-29 cell lines respectively. Further, studies like Hoechst staining and DNA fragmentation assay strengthened the preliminary results and ascertained the role of apoptosis induction as the mechanism of action of the synthesized compounds. Anti-inflammatory assessment for the three most potent anticancer compounds was performed by protein albumin denaturation assay and red blood cell membrane stabilizing assay. On the whole, it was observed that all the synthesized compounds demonstrated significant anti-inflammatory potential in addition to anticancer effects.

Acknowledgements

Mr. Mohemmed Faraz Khan would like to acknowledge University Grant Commission (UGC), Government of India as he is the recipient of Research Fellowship of the UGC-MANF scheme of UGC, Government of India. The authors would also like to thank Jamia Hamdard, New Delhi and DST-PURSE, Government of India.

Conflict of Interest

Authors declare no conflict of interest.

References

1. M. Taha, S.A.A. Shah, M. Afifi, M. Zulkeflee, S. Sultan, A. Wadood, F. Rahim, N.H. Ismail, Morpholine hydrazone scaffold: synthesis, anticancer activity and docking studies, *Chin. Chem. Lett.* 28 (2017) 607-611.
2. C.-J. Liu, S.-L. Yu, Y.-P. Liu, X.-J. Dai, Y. Wu, R.-J. Li, J.-C. Tao, Synthesis, cytotoxic activity evaluation and HQSAR study of novel isosteviol derivatives as potential anticancer agents, *Eur. J. Med. Chem.* 15 (2016) 26-40.
3. P. Wang, J. Cai, J. Chen, M. Ji, Synthesis and anticancer activities of ceritinib analogs modified in the terminal piperidine ring, *Eur. J. Med. Chem.* 93 (2015) 1-8.
4. R.R. Ruddarraju, A.C. Murugulla, R. Kotla, M.C.B. Tirumalasetty, R. Wudayagiri, S. Donthabakthuni, R. Marjou, K. Baburao, L.S. Parasa, Design, synthesis, anticancer, antimicrobial activities and molecular docking studies of theophylline containing 1,2,3-triazoles with variant nucleoside derivatives, *Eur. J. Med. Chem.* 123 (2016) 379-396.
5. I. Chaaban, E.S.M. El Khawass, H.A. Abd El Razik, N.S. El Salamouni, M. Redono-Horcajo, I. Barasoain, J.F. Diaz, J. Yli-Kauhaluoma, V.M. Moreira, Synthesis and biological evaluation of new oxadiazoline-substituted naphthyl acetates anticancer agents, *Eur. J. Med. Chem.* 87 (2014) 805-813.
6. B.-Z. Qian, Inflammation fires up cancer metastasis, *Semin. Cancer Biol.* 47 (2017) 170-176.
7. H. Marusawa, B.J. Jenkins, Inflammation and gastrointestinal cancer: an overview, *Cancer Lett.* 345 (2014), 153-156.
8. J.K. Kundu, Y.-J. Surh, Emerging venues linking inflammation and cancer, *Free Radic. Biol. Med.* 52 (2012) 2013-2037.
9. J. Qin, W. Wang, R. Zhng, Novel natural product therapeutics targeting both inflammation and cancer, *Chin. J. Nat. Med.* 15 (2017) 401-416.
10. B.B. Aggarwal, S. Shishodia, S.K. Sandur, M.K. Pandey, G. Sethi, Inflammation and cancer: How hot is the link?, *Biochem. Pharmacol.* 72 (2006) 1605-1621.
11. J.K. Kundu, Y.-J. Surh, Inflammation: Gearing the journey to cancer, *Mutat. Res.* 659 (2008) 15-30.
12. R.J. Moore, D.M. Owens, G. Stamp, C. Arnott, F. Burke, N. East, H. Holdsworth, L. Turner, B. Rollins, M. Pasparakis, G. Kollias, F. Balkwill, Mice deficient in tumor necrosis factor- α are resistant to skin carcinogenesis, *Nat. Med.* 5 (1999) 828-831.

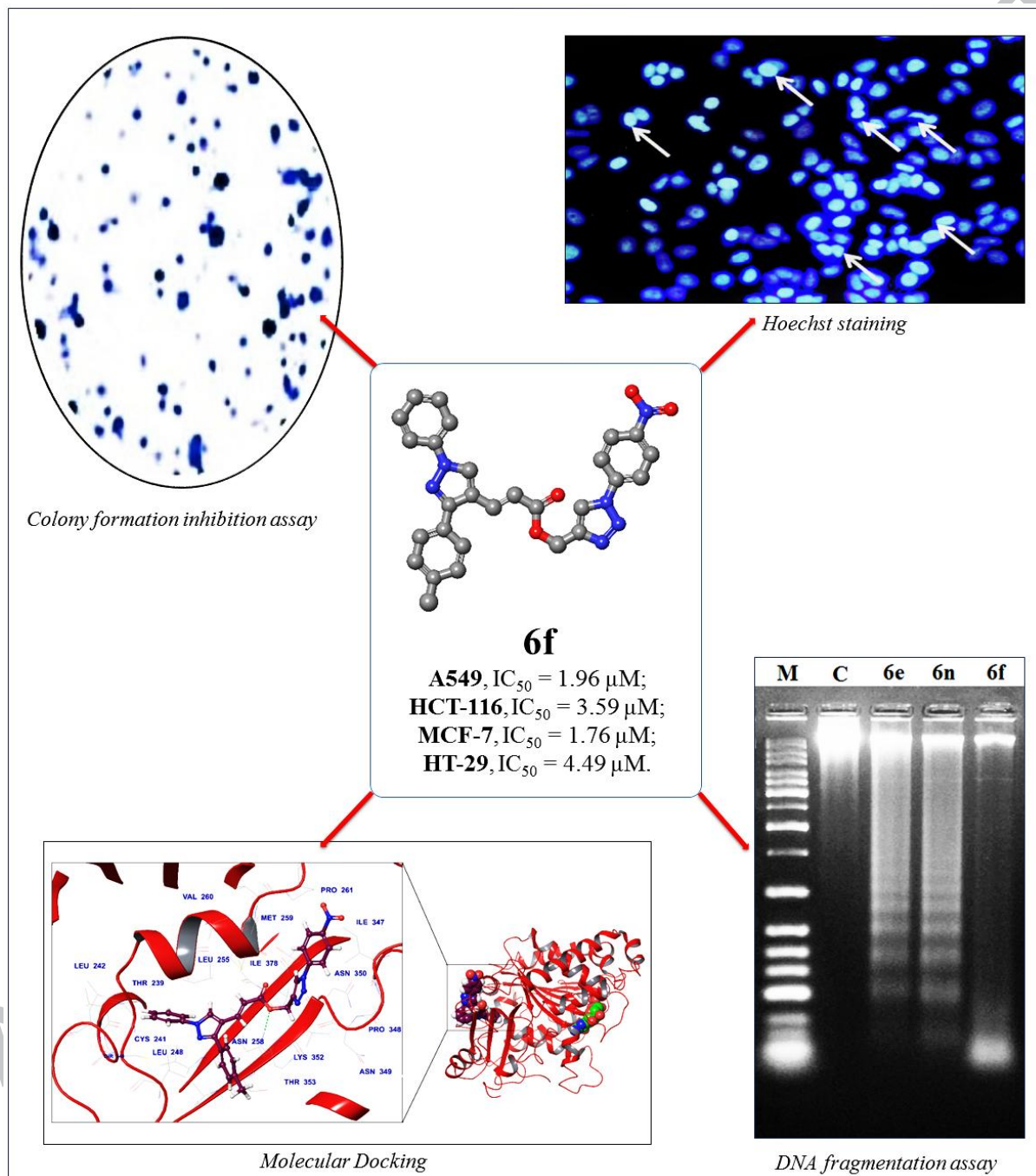
13. Y. Wu, B.P. Zhou, Inflammation: a driving force speeds cancer metastasis, *Cell Cycle*. 8 (2009) 3267-3273.
14. C. Brandt, B.K. Pedersen, The role of exercise-induced myokines in muscle homeostasis and the defense against chronic diseases, *J. Biomed. Biotechnol.* 2010 (2010) Article ID 520258, 1-6. doi: 10.1155/2010/520258.
15. K. Aleksandrova, M. Jenab, H. Boeing, E. Jansen, H.B. Bueno-de-Mesquita, S. Rinaldi, E. Riboli, K. Overvad, C.C. Dahm, A. Olsen, A. Tjønneland, M.-C. Boutron-Ruault, F. Clavel-Chapelon, S. Morois, D. Palli, V. Krogh, R. Tumino, P. Vineis, S. Panico, R. Kaaks, S. Rohrmann, A. Trichopoulou, P. Lagiou, D. Trichopoulos, F.J.B. van Duijnhoven, A.M. Leufkens, P.H. Peeters, L. Rodríguez, C. Bonet, M.-J. Sánchez, M. Dorronsoro, C. Navarro, A. Barricarte, R. Palmqvist, G. Hallmans, K.-T. Khaw, N. Wareham, N.E. Allen, E. Spencer, D. Romaguera, T. Norat, T. Pischon, Circulating C-Reactive Protein Concentrations and Risks of Colon and Rectal Cancer: A Nested Case-Control Study Within the European Prospective Investigation into Cancer and Nutrition, *A. J. Epidemiol.* 172 (2010) 407–418.
16. E. Piazzuelo, A. Lanas, NSAIDS and gastrointestinal cancer, *Prostaglandins Other Lipid Mediat.* 120 (2015) 91–96.
17. J.V. Faria, P.F. Vegi, A.G.C. Miguita, M.S. Santos, N. Boechat, A.M.R. Bernardino, Recently reported biological activities of pyrazole compounds, *Bioorg. Med. Chem.* 25 (2017) 5891-5903.
18. M.F. Khan, M.M. Alam, G. Verma, W. Akhtar, M. Akhter, M. Shaquiquzzaman, The therapeutic voyage of pyrazole and its analogs: A review, *Eur. J. Med. Chem.* 120 (2016) 170-201.
19. D. Dheer, V. Singh, R. Shankar, Medicinal attributes of 1,2,3-triazoles: Current developments, *Bioorg. Chem.* 71 (2017) 30–54.
20. B. Caliskan, A. Yilmaz, I. Evren, S. Menevse, O. Uludag, E. Banoglu, Synthesis and evaluation of analgesic, anti-inflammatory, and anticancer activities of new pyrazole-3(5)-carboxylic acid derivatives, *Med. Chem. Res.* 22 (2013) 782–793.
21. S.M. Sondhi, S. Kumar, N. Kumar, P. Roy, Synthesis anti-inflammatory and anticancer activity evaluation of some pyrazole and oxadiazole derivatives, *Med. Chem. Res.* 21 (2012) 3043–3052.
22. P.S. Rao, C. Kurumurthy, B. Veeraswamy, G.S. Kumar, Y. Poornachandra, C.G. Kumar, S.B. Vasamsetti, S. Kotamraju, B. Narsaiah, Synthesis of novel 1,2,3-triazole

- substituted-N-alkyl/aryl nitron derivatives, their anti-inflammatory and anticancer activity, *Eur. J. Med. Chem.* 80 (2014) 184-191.
23. S. Haider, M.S. Alam, H. Hamid, S. Shafi, A. Dhulap, F. Hussain, P. Alam, S. Umar, M.A.Q. Pasha, S. Bano, S. Nazreen, Y. Ali, C. Kharbanda, Synthesis of novel 2-mercaptobenzoxazole based 1,2,3-triazoles as inhibitors of proinflammatory cytokines and suppressors of COX-2 gene expression, *Eur. J. Med. Chem.* 81 (2014) 204-217.
24. T.S. Reddy, V.G. Reddy, H. Kulhari, R. Shukla, A. Kamal, V. Bansal, Synthesis of (Z)-1-(1,3-diphenyl-1H-pyrazol-4-yl)-3-(phenylamino)prop-2-en-1-one derivatives as potential anticancer and apoptosis inducing agents, *Eur. J. Med. Chem.* 117 (2016) 157-166.
25. S.Y. Jadhav, S.P. Shirame, S.D. Kulkarni, S.B. Patil, S.K. Pasale, R.B. Bhosale, PEG mediated synthesis and pharmacological evaluation of some fluoro substituted pyrazoline derivatives as antiinflammatory and analgesic agents, *Bioorg. Med. Chem. Lett.* 23 (2013) 2575–2578.
26. S.P. Shaik, V.L. Nayak, F. Sultana, A.V.S. Rao, A.B. Shaik, K.S. Babu, A. Kamal, Design and synthesis of imidazo[2,1-b]thiazole linked triazole conjugates: Microtubule-destabilizing agents, *Eur. J. Med. Chem.* 126 (2017) 36-51.
27. P.S. Rao, C. Kurumurthy, B. Veeraswamy, G.S. Kumar, Y. Poornachandra, C.G. Kumar, S.B. Vasamsetti, S. Kotamraju, B. Narsaiah, Synthesis of novel 1,2,3-triazole substituted-N-alkyl/aryl nitron derivatives, their anti-inflammatory and anticancer activity, *Eur. J. Med. Chem.* 80 (2014) 184-191.
28. T.S. Reddy, H. Kulhari, V.G. Reddy, A.V.S. Rao, V. Bansal, A. Kamal, R. Shukla, Synthesis and biological evaluation of pyrazolo-triazole hybrids as cytotoxic and apoptosis inducing agents, *Org. Biomol. Chem.* 13 (2015) 10136-10149.
29. V.G. Reddy, T.S. Reddy, V.L. Nayak, B. Prasad, A.P. Reddy, A. Ravikumar, S. Taj, A. Kamal, Design, synthesis and biological evaluation of N-((1-benzyl-1H-1,2,3-triazol-4-yl)methyl)-1,3-diphenyl-1H-pyrazole-4-carboxamides as CDK1/Cdc2 inhibitors, *Eur. J. Med. Chem.* 122 (2016) 164-177.
30. C. Dayakar, B.S. Kumar, G. Sneha, G. Sagarika, K. Meghana, S. Ramakrishna, R.S. Prakasham, B.C. Raju, Synthesis, pharmacological activities and molecular docking studies of pyrazolyltriazoles as anti-bacterial and anti-inflammatory agents, *Bioorg. Med. Chem.* 25 (2017) 5678–5691.

31. S. Fang, L. Chen, M. Yu, B. Cheng, Y. Lin, S.L. Morris-Natschke, K.-H. Lee, Q. Gu, J. Xu, Synthesis, antitumor activity, and mechanism of action of 6-acrylic phenethyl ester-2-pyranone derivatives, *Org. Biomol. Chem.* 13 (2015) 4714-4726.
32. K.S. Joshi, M. Sivakumar, V.S. Aware, V.S. Wagh, A. Deshpande, A. G. Sarde, S. Sharma, Anti cancer use of caffeic acid and derivatives, EP 2061452 B1, Oct 26, (2011).
33. V.K. Redasani, A.B. Shinde, S.J. Surana, Anti-Inflammatory and Gastroprotective Evaluation of Prodrugs of Piroxicam, *Ulcers*, 2014 (2014) Article ID 729754, 1-4. <http://dx.doi.org/10.1155/2014/729754>.
34. G. Verma, G. Chashoo, A. Ali, M.F. Khan, W. Akhtar, I. Ali, M. Akhtar, M.M. Alam, M. Shaquiquzzaman, Synthesis of pyrazole acrylic acid based oxadiazole and amide derivatives as antimalarial and anticancer agents, *Bioorg. Chem.* 77 (2018) 106–124.
35. M.P. Reddy, G.S.K. Rao. Applications of the Vilsmeier reaction. 13. Vilsmeier approach to polycyclic aromatic hydrocarbons. *J. Org. Chem.* 46 (1981) 5371-5733.
36. A.M.A.D. Souza, V.L.D.M. Guarda, L.F.C.D.C. Leite, J.M.B. Filho, M.D.C.A.D. Lima, S.L. G.I.D.R. Pitta. On the application of Knoevenagel Condensation for the synthesis of benzylidene benzothiazine compounds and structural study. *Quim Nova.* 29 (2006), 1106-1109.
37. K.E. Kolb, K.W. Field, P.F. Schatz. One step synthesis of cinnamic acids using malonic acid: the Verley-Doebner modification of the Knoevenagel condensation. *J. Chem. Edu.* A304.
38. T. Batool, N. Rasool, Y. Gull, M. Noreen, F. Nasim, A. Yaqoob, M. Zubair, U.A. Rana, S. U.-D. Khan, M. Zia-Ul-Haq, H.Z.E. Jaafar, A Convenient Method for the Synthesis of (Prop-2-Ynyloxy)Benzene Derivatives via Reaction with Propargyl Bromide, Their Optimization, Scope and Biological Evaluation, *PLoS ONE*, 9 (2014): e115457. doi:10.1371/journal.pone.0115457
39. Ksenia V. Kutonova, Marina E. Trusova, Pavel S. Postnikov, Victor D. Filimonov, Joseph Parello. A Simple and Effective Synthesis of Aryl Azides via Arenediazonium Tosylates, *Synthesis*. 2013, 45, 2706–2710.
40. S.B. Ferreira, A.C.R. Soderro, M.F.C. Cardoso, E.S. Lima, C.R. Kaiser, F.P. Silva Jr., V.F. Ferreira. Synthesis, Biological Activity, and Molecular Modeling Studies of 1H-1,2,3-Triazole Derivatives of Carbohydrates as α -Glucosidases Inhibitors. *J. Med. Chem.*, 53 (2010) 2364–2375.
41. N.A.P. Franken, H.M. Rodermond, J. Stap, J. Haveman, C.V. Bree. Clonogenic assay of cells *in vitro*, *Nat. Protoc.* 1 (2006) 2315-2319.

42. Q. Hou, T. Zhao, H. Zhang, H. Lu, Q. Zhang, L. Sun, Z. Fan. Granzyme H induces apoptosis of target tumor cells characterized by DNA fragmentation and Bid-dependent mitochondrial damage, *Mol. Immunol.* 45 (2008) 1044-1055.
43. M.J. Naim, M.J. Alam, F. Nawaz, V.G.M. Naidu, S. Aghaz, M. Sahu, N. Siddiqui, O. Alam. Synthesis, molecular docking and anti-diabetic evaluation of 2,4-thiazolidinedione based amide derivatives, *Bioorg. Chem.* 73 (2017) 24-36.
44. J.J. Vora, S.B. Vasava, K.C. Parmar, S.K. Chauhan, S.S. Sharma. Synthesis, spectral and microbial studies of some novel Schiff base derivatives of 4-Methylpyridin-2-amine, *J. Chem.* 6 (2009) 1205-1210.
45. W. Voigt. Sulforhodamine B assay and chemosensitivity, *Methods Mol Med*, 2005, 110, 39-48.
46. J. Stamos, M.X. Sliwkowski, C. Eigenbrot. Structure of the epidermal growth factor receptor kinase domain alone and in complex with a 4-anilinoquinazoline inhibitor, *J. Biol. Chem.* 277, 46265-46272.
47. G.M. Sastry, M. Adzhigirey, T. Day, R. Annabhimoju, W. Sherman. Protein and ligand preparation: parameters, protocols and influence on virtual screening enrichments, *J. Comput. Aided Mol. Des.* 27, 221-234.

Graphical Abstract



Highlights

- 1,2,3-triazole linked 3-(1,3-diphenyl-1*H*-pyrazol-4-yl)acrylates were synthesized.
- **6e**, **6f** and **6n** inhibited proliferation of cell lines MCF-7, A549, HCT-116 & HT-29.
- **6f** showed IC₅₀ values of 1.96(A549), 3.59(HCT-116), 1.76(MCF-7) & 4.49(HT-29) μ M.
- Compounds **6e**, **6f** and **6n** were found to induce apoptosis.
- Anti-inflammatory activity for these compounds was also evaluated.